# Finite Element Analysis of Compressive Stress-Strain Relations in Elastic Materials for Seat Foundation

Weikang Li,[a] Xiaohong Yu,[a] Xiaoyi Hu,[a] Onder Tor,[b] Jilei Zhang,[c] Ting Zhang,[d] Wei Qi,[a] and Lingling Hu [a,*]

Elastic materials for seat foundations come in a variety of materials, shapes, and dimensions. However, it is difficult to measure the stress-strain relationships of many elastic material combinations by conventional uniaxial compression tests. This study investigated the stress-strain relations of elastic material combinations for foam foundations using finite element analysis (FEA). First, the stress-strain relations of single-layer polymer foams and a combination of double-layer polymer foams with covering were quantified by uniaxial compression tests, and axial tensile tests quantified the properties of the covering material of the fabric. Then, based on the Ogden foam and Ogden constitutive equation of Ansys Workbench 19.2, the test data of single-layer polymer foams and covering were fitted by a non-linear least square method, and a combination of double-layer polymer foams with the covering is predicted by FEA. When the strain was 10% to 65%, the stress error between FEA and test results dropped from 95.68% to -5.08%.

*DOI: 10.15376/biores.18.4.7731-7744*

*Keywords: Stress-strain; Seat foundation; Ogden foam; Finite element analysis*

*Contact information: a: Department of Furniture Design and Engineering, Zhejiang A&F University, Hangzhou, China; b: Department of Forest Industry Engineering, Kastamonu University, Kastamonu, Turkey; c: Department of Sustainable Bioproducts, Mississippi State University, Starkville, MS, USA; d: Research and Development Center, Xilinmen Furniture Co., Ltd., Shaoxing, China;*
** Corresponding author: radiant00@163.com*

## INTRODUCTION

The combination of elastic materials used for the seat foam foundation determines the sitting experience (Hu *et al.* 2015; Li 2018; Hu *et al*. 2020). Common elastic materials, such as polymer foams, springs, bandages, and fabrics, are widely used in the applications of furniture, automobile, and many other industries. Regarding the combination of elastic materials, seat manufacturers and designers have long relied on uniaxial compression tests and workers' experience. However, it is difficult to systematically quantify the stress-strain relations of a wide range of elastic material combinations through conventional uniaxial compression tests. In recent years, finite element analysis (FEA) has become famous for its intuitive and timely application in modeling engineering mechanics. Through creating many simulation models, FEA can solve boundary value problems in different operating situations (Chen and Cai 2018; Zeng *et al*. 2021). However, analysis of one such combination trace can replace many tests in determining seat foundation curves.

Several studies on seat comfort have used finite element development programs or fitting tools to generate constitutive model parameters and then simulate the mechanical behavior of single-layer polymer foams for automobile seats (Du *et al*. 2013; Gao *et al*. 2019; Zhang *et al*. 2019). Kumar *et al*. (2019) developed the hyperelastic model parameters representing the stress-strain curve of single-layer polymer foam for compressive loading. Then, various other parameters, such as stiffness and thickness were considered to

investigate seat comfort using FEA (Schrodt *et al*. 2005). Schrodt *et al.* (2005) simulated the stress-strain relations of a single-layer polymer foam by the parameters of the second-order strain energy function. Briody *et al*. (2011) used the non-linear least-squares optimization program in Abaqus. They fitted the compression test data of single-layer polyurethane foam using the strain energy equation of the hyperfoam (Ogden) model. Chou *et al*. (1995) investigated the stress-strain relations of single-layer foam with various foam models of LS-DYNA 3D; numerous simulations were carried out for foams subjected to different loading conditions. By combining the advanced measurement techniques, non-traditional experimental setup, numerical modeling (FE model) and inverse analysis one can capture all nine elastic properties of single-layer polymer foam from just two or three tests (Chuda-Kowalska *et al*. 2015). Although FEA has well evaluated the mechanical properties of single-layer foams, studies on the mechanical properties of double-layer or multi-layer foams are limited.

Polymeric foam and coverings belong to the elastomer category. The hyperelastic constitutive model is widely used in simulation to characterize the stress-strain relations of elastomers (Fernández *et al*. 2018; Heczko and Kottner 2018; Masrar and Ettaouil 2021). The non-linear stress-strain relations of elastic materials, such as seat cushions and hyperelastic foams, are often described by the Ogden model based on stretch ratio (Ogden 1972, 1984). Liu and Subhash (2005) developed a five-parameter constitutive model for the foam in single and multiple compression tests. They used the non-linear least square approach to fit the test data. The results showed that the five-parameter constitutive model could accurately predict the overall stress-strain response of the polymer foam (Liu *et al*. 2004; Liu and Subhash 2005). Studies have been performed on the stress-strain response of polymer foam using the crushable foam model and the low-density foam model; these approaches made it possible to calculate the force-deformation under compression loads and unloading (Ozturk and Anlas 2007, 2010). Mills and Gilchrist (2000) used the Ogden model to predict the polyurethane foam response for both plane strain indentation and the axisymmetric indentation force deflection (IFD), and the results showed that the relative indentation forces were about 20% lower than the experimental values.

Many researchers have presented the stress-strain constitutive model and the corresponding parameter-matching method for elastic materials, such as polymer foam, in the field of automobile seats, but few methods for elastic materials have been used in seat foundations of furniture. In addition, more attention has been paid in the literature to the compressive yield of single-layer polymer foam under uniaxial compression or multiaxial compression, but FEA research on multi-layer polymer foam foundations is limited. This study investigates the stress-strain of single-layer polymer foams and combination of double-layer polymer foams with covering under uniaxial compression tests. It examines the stress-strain relations of elastic materials on seat foundations using FEA.

## EXPERIMENTAL

### Materials

Polymer foams and coverings are most commonly used for seat foundations. To analyze stress-strain of the seat foundation, the polyurethane foam, polyether-polyol foam, and fabric were chosen in experimental tests. The polyether-polyol foam is designated as Foam A ($F_A$, density of 24.88 kg/m$^3$), and the polyurethane foam is designated as Foam B ($F_B$, density of 38.76 kg/m$^3$). The tested elastic materials are listed in Table 1. The size of single-layer polymer foams is 100 mm × 100 mm × 50 mm (length, breadth, and thickness), and 740 mm × 740 mm × 200 mm (length, breadth, and thickness) for double-layer polymer

foams with covering. In addition, a layer of 25-mm-thick silk wadding was inserted between the polymer foams and covering in the combination of seat foundation elastic material process, as depicted in Fig. 1.

**Table 1.** Tested Elastic Materials for Foam Foundations

| Foam Foundation Type | Implication | Combinations | Abbreviations |
|---|---|---|---|
| Single-layer polymer foams (Small size foam) | / | / | $F_A$, $F_B$ |
| Double-layer polymer foams with covering | Double-layer foams covered with silk wadding and fabric covering | Foam A + Foam B + Fabric | $F_{AB}F$ |

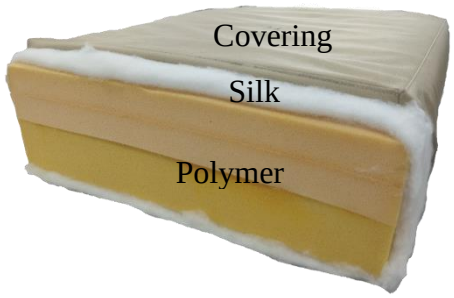


**Fig. 1.** The combination of double-layer polymer foams, silk wadding, and covering

## Experimental Tests

In accordance with the American Society for Testing of Materials polymer foam test standard (ASTM D3574-B1 (2003), the uniaxial compression tests with an aluminum disk with a diameter of 200 mm were performed on $F_A$ and $F_B$ with a dimension of 100 mm × 100 mm × 50 mm (length, breadth, and thickness) on the HD-F750 type mechanical tester (Haida, Dongguan, China) with three replicates of each. In addition, according to EN 1957 (2000), FABF with dimensions of 740 mm × 740 mm × 200 mm (length, breadth, and thickness) on the TST-CD001 type mechanical tester (TST, Fujian, China) were tested with three replicates of each. An aluminum disk with a diameter of 350 mm was used for the tests, and the specimen was compressed to 65% of the thickness at a uniform speed of 100 mm/min. The stress-strain relation (Elastic modulus: $E_1$, $E_2$, $E_3$) of $F_A$ and $F_B$ were investigated based on a previously reported methods (Hu *et al*. 2020), as shown in Table 2 and Fig. 2. The stress values of strain (the ratio of compression amount to thickness of the specimen) for 10%, 15%, 20%, 25%, 30%, 35%, 40%, 45%, 50%, 55%, 60%, and 65% were selected, and the results are reported in Table 5.

**Table 2.** $E_1$, $E_2$, and $E_3$ Values for Stress-Strain Relation of $F_A$ and $F_B$

| Foam | $E_1$ (KPa) | $E_2$ (KPa) | $E_3$ (KPa) |
|---|---|---|---|
| | 0% to 5% strain | 5% to 50% strain | 50 to 70% strain |
| $F_A$ | 26.4 | 1.7 | 31.5 |
| $F_B$ | 59.2 | 4.5 | 26.4 |

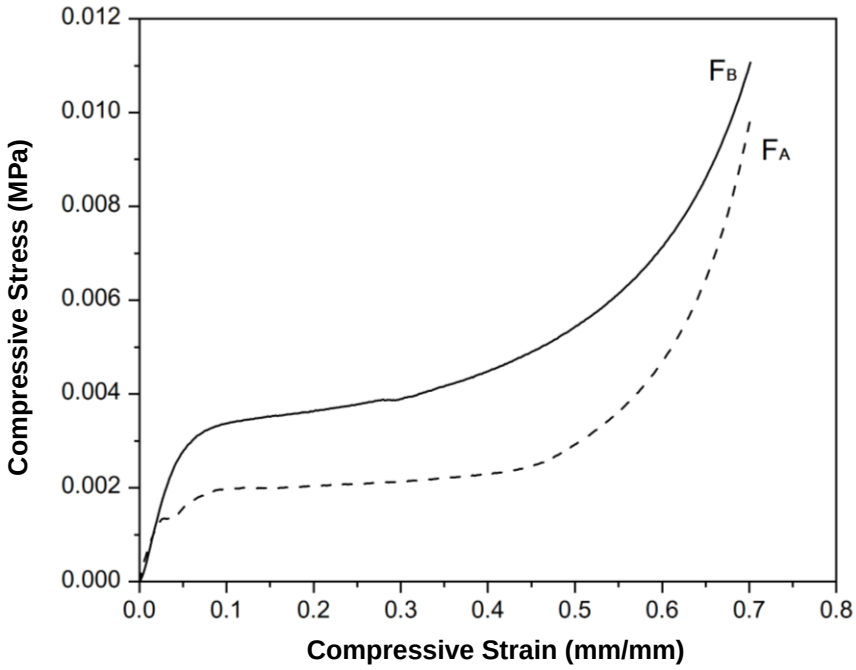


**Fig. 2.** The stress-strain relation of $F_A$ and $F_B$

Based on GB/T 3923.1 (2013), the axial textile tests were conducted for the fabric covering specimens with dimensions of 100 mm × 25 mm were performed using a CMT5967 materials testing system (INSTRON, Norwood, MA, USA). The two ends of the fabric specimens were fixed with clamps to ensure that the covering specimens did not slip. The axial tensile rate during loading was 100 mm/min, and the maximum load was 200 N. Each covering specimen was tested five times. The stress-strain curves of the covering are shown in Fig. 3.

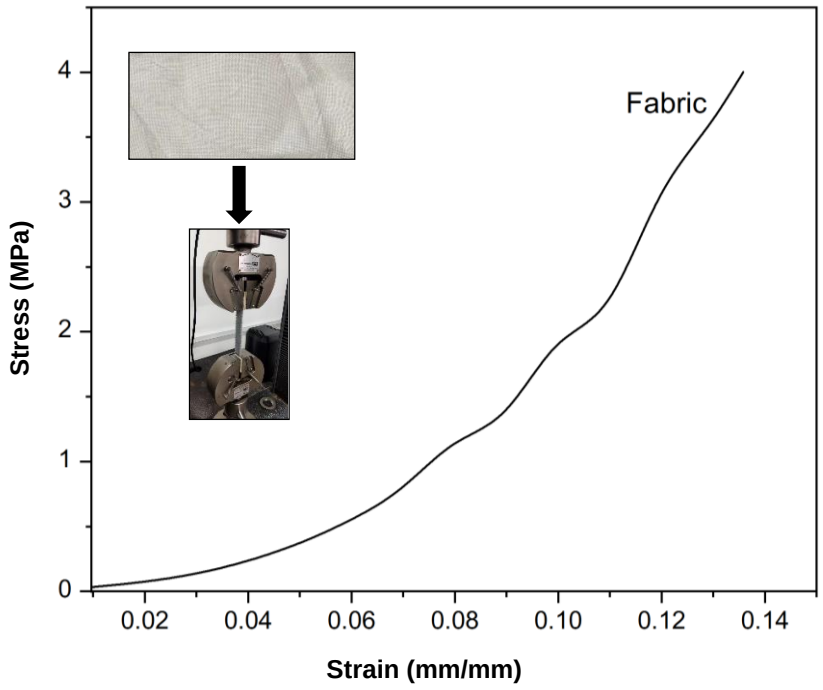


**Fig. 3.** Stress-strain curves of fabric materials

## Finite Element Analysis of Elastic Materials for Seat Foundation

*Definition of polymer foam*

The stress-strain relations of polymer foam can be described in Ansys Workbench 19.2 by the Ogden Foam constitutive model (Zhang *et al*. 2005). In this model, the potential energy *W* of elastic deformation was used to represent the elasticity of the material. The volume term and the partial term are completely connected due to the almost complete compressibility of the elastic foam. The strain energy potential was derived by Eq. 1, which was based on the principal stretches of the left Cauchy-Green tensor (ANSYS Workbench Help), as follows:

$$W=\sum_{i=1}^{N}\frac{u_i}{\alpha_i}(J^{\alpha_i/3}(\overline{\lambda_1}^{\alpha_i}+\overline{\lambda_2}^{\alpha_i}+\overline{\lambda_3}^{\alpha_i})-3)+\sum_{i=1}^{N}\frac{u_i}{\alpha_i\beta_i}(J^{-\alpha_i\beta_i}-1) \quad (1)$$

The parameters (i = 1, 2,...,n) are defined as follows: $u_i$ , $\alpha_i$ is the fundamental parameter of the material, $\beta_i$ is the compressible coefficient, $J$ is the elastic volume ratio, $\lambda_i$ is the principal stretches, and $N$ is the order of the model. To ensure that the calculation in the Ansys Workbench 19.2 is stable, $u_i \cdot \alpha_i$ should be greater than zero.

The initial shear modulus $u$ is defined by:

$$u=\frac{\sum_{i=1}^{N}\frac{u_i}{\alpha_i}}{2} \quad (2)$$

The transverse stretches $\lambda_1$ and $\lambda_3$ were negligible during the uniaxial tensile test. Therefore, the derivative of the strain energy potential $W$ in the direction of the main stretch is calculated using the simplified Eq. 1. As a result, the nominal stress in the load direction can therefore be calculated as follows:

$$\sigma=\sum_{i=1}^{N}(\frac{2u_i}{3\lambda_2}\cdot J^{\alpha_i/3}+\frac{4u_i}{3\lambda_2}\cdot J^{\alpha_i/3}\cdot\lambda_2{}^{\alpha_i}-\frac{u_i}{\lambda_2}\cdot J^{-\alpha_i\beta_i}) \quad (3)$$

In Eq. 3, the principal stretch can be expressed as:

$$\lambda_2=\lambda=\frac{L+\Delta L}{L}=1+\varepsilon \quad (4)$$

The stress-strain should be defined as negative because the single-layer polymer foam was evaluated under uniaxial compression in this study. The stretching quantity in the $\lambda_1$ and $\lambda_3$ direction of the polymer foam is also insignificant for extremely compressible foam materials with a Poisson's ratio of zero (Briody *et al*. 2011, 2012) resulting in $\lambda_2=\lambda$ and $\lambda_1=\lambda_3=1$. The elastic volume ratio is given by Eq. 5:

$$J=\lambda_1\lambda_2\lambda_3 \quad (5)$$

The compressible parameter $\beta_i$ is defined as:

$$\beta_i=\frac{v_i}{1-2v_i} \quad (6)$$

Because Poisson's ratio $v_i$ of the polymer foam is zero, the compressibility coefficient $\beta_i$ is also defined as zero. The elastic volume ratio $J$ can be defined as the stretch ratio in the direction of $\lambda_2$ of the uniaxial compression test. This gives Eq. 7,

$$J=\frac{v_0}{v}=\frac{L-\Delta L}{L} \quad (7)$$

where $v_0$ is the volume ($mm^3$) of the polymer foam specimen after deformation, $v$ is the original volume ($mm^3$) of the polymer foam specimen, $L$ is the original length (mm) of the polymer foam specimen, and $\Delta L$ is the axial pressure (mm) of the polymer foam specimen. The stretch ratio in the direction of $\lambda_2$ under uniaxial compression of polymer foam can alternatively be expressed as:

$$\lambda_2 = \lambda = \frac{L - \Delta L}{L} = 1 - \varepsilon \tag{8}$$

To calculate the derivative of strain to obtain the stress-strain relations of polymer foam under uniaxial compression, Eqs. 7 and 8 are substituted into Eq. 1 to assist the establishment of the connection with the test data as follows:

$$\sigma_i = \frac{\partial W}{\partial \varepsilon} = \sum_{i=1}^{N} \left( -\frac{2u_i}{3} \cdot (1-\varepsilon)^{\frac{\alpha_i}{3}-1} - \frac{4u_i}{3} \cdot (1-\varepsilon)^{\frac{4}{3}\alpha_i - 1} + u_i \cdot (1-\varepsilon)^{-\alpha_i \beta_i - 1} \right) \tag{8}$$

In the present work, a second order (*i.e.*, N = 2) strain energy Ogden foam potential function is used, which gives:

$$\sigma_{(N=2)} = -\frac{2u_1}{3} \cdot (1-\varepsilon)^{\frac{\alpha_1}{3}-1} - \frac{4u_1}{3} \cdot (1-\varepsilon)^{\frac{4}{3}\alpha_1 - 1} + u_1 \cdot (1-\varepsilon)^{-\alpha_1 \beta_1 - 1} - \frac{2u_2}{3} \cdot (1-\varepsilon)^{\frac{\alpha_2}{3}-1} - \frac{4u_2}{3} \cdot (1-\varepsilon)^{\frac{4}{3}\alpha_2 - 1} + u_2 \cdot (1-\varepsilon)^{-\alpha_2 \beta_2 - 1} \tag{9}$$

The parameters cannot be predicted from the polymer foam properties, the foam density, and the deformation mechanisms. Instead, they must be calculated by curve-fitting experimental data (Fig. 2). The Ogden foam model of second order (Mohanty and Mahapatra 2014; Maiti *et al*. 2019) is sufficient to fit the experimental data (Fig. 4), and the model parameters are shown in Table 3.

**Table 3.** Foam Properties of Ogden Foam 2nd Order for $F_A$ and $F_B$ (Eq. 9)

| | $u_1$ (kPa) | $\alpha_1$ | $\beta_1$ | $u_2$ (kPa) | $\alpha_2$ | $\beta_2$ | Goodness of Fit ($R^2$) |
|---|---|---|---|---|---|---|---|
| $F_A$ | 1.786 | 202.4 | 0 | 0.7071 | 0.9901 | 0 | 0.85 |
| $F_B$ | 1.056 | 0.045 | 0 | 3.665 | 163.9 | 0 | 0.92 |

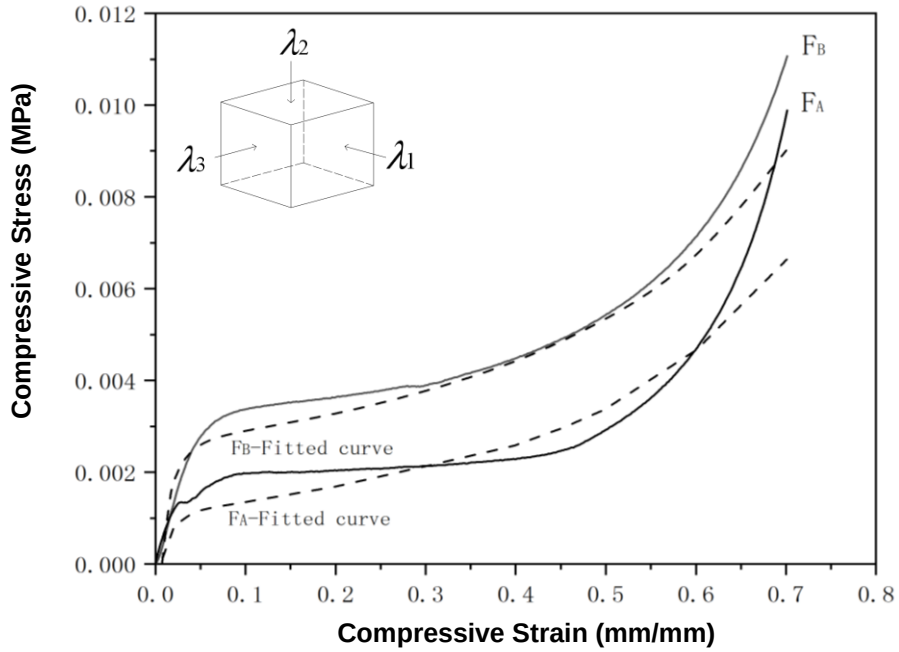


**Fig. 4.** Fitting curves for $F_A$ and $F_B$ were calculated using Eq 9.

*Definition of covering materials*

In general, the Ogden constitutive model is well suited to solving the problem of large strains of elastic materials. The Ogden hyperelastic constitutive model was used in this study to describe elastic material in Ansys Workbench 19.2 (ANSYS Inc., Canonsburg, PA, USA). The strain energy potential function Eq. 10, similar to Eq. 1, is also based on the principal stretches of the Zuocchi-Green strain tensor, and its form is defined as follows:

$$W = \sum_{i=1}^{N} \frac{u_i}{\alpha_i} (\overline{\lambda_1}^{\alpha_i} + \overline{\lambda_2}^{\alpha_i} + \overline{\lambda_3}^{\alpha_i} - 3) + \sum_{k=1}^{N} \frac{1}{d_k} (J-1)^{2k} \quad (10)$$

The $d_k$ in Eq. 9 is the incompressible coefficient. Hyperelastic materials are incompressible materials, which means that their volume does not change during compression. Consequently, $J = \lambda_1\lambda_2\lambda_3 = 1$. The deformation of Ogden's hyperelastic constitutive model is defined as follows:

$$W = \sum_{i=1}^{N} \frac{u_i}{\alpha_i} (\overline{\lambda_1}^{\alpha_i} + \overline{\lambda_2}^{\alpha_i} + \overline{\lambda_3}^{\alpha_i} - 3) \quad (11)$$

The experimental stress-strain data for fabric is imported into the Ogden hyperelastic constitutive model, and the test data are fitted using the fitting tool (Error norm for fit) in Ansys Workbench 19.2 (Table 4). The incompressible coefficient $d_k$ is defined as 0 in the fitting process as shown in Eq. 11.

**Table 4.** Foam Material Properties of Ogden 1st Order for Covering

| Type of Covering | $u_1$ (kPa) | $\alpha_1$ | $d_1$ |
|---|---|---|---|
| Fabric(N = 1) | 72.4 | 33.974 | 0 |

*Model construction of seat foundation*

The compression behavior for the FABF is a large non-linear deformation. When calculating the large deformation of the composite compression in FEA, the shear stress generated at the contact point between the polymer foam sidewall and the covering can easily lead to problems of stress singularity or non-convergence of the results. Defining proper boundary conditions and adjusting the mesh size in FEA can solve this problem. The covering on the side of polymer foam has little effect on the seat support ability and is therefore ignored in the simulation. In addition, a layer of 50-mm-thick elastic foam ($u_1$ = 1000 Pa, $\alpha_1 = 1$, $\beta_1 = 0$) is constructed to replace the compressibility of the silk wadding.

*Mesh division and boundary conditions*

The hexahedral mesh was used to improve the accuracy of simulation results in this study (Fig. 5 ). The contacts of the covering, polymer foam, and aluminum disk are set as bonded (glue connection between polymer foam) in the FEA, which means that the contact surfaces remain in initial contact with each other and there is no relative sliding or no separation. The bottom of the foam foundation is fixed support from all directions, and the aluminum disk is designed to achieve a compressive strain of 65% combination thickness. In order to analyze the influence of mesh size on compressive stress value in FABF, the sensitivity of mesh size (65 to 45 mm) of polymer foam was simulated. Table 5 shows that the stress error corresponding to 0.1 to 0.65 strain of polymer foam is not more than 5.10%.

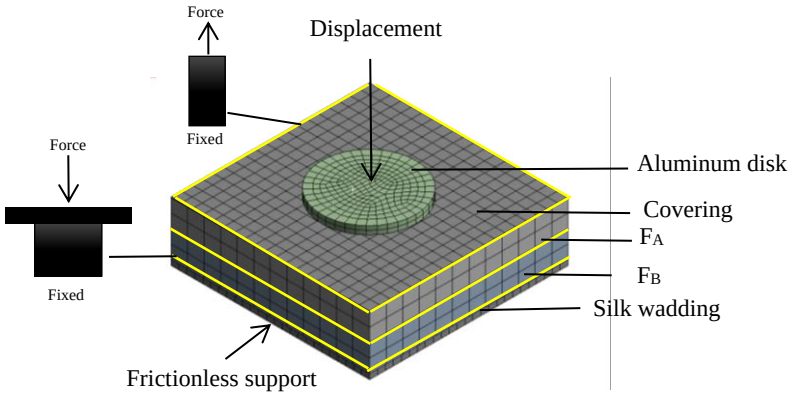


**Fig. 5.** Finite element model of $F_{AB}F$

**Table 5.** The Influence of $F_A$ ($F_B$) Mesh Size on Simulation Results in $F_{AB}F$

| Strain (mm/mm) | Stress (kPa) | | | | |
|---|---|---|---|---|---|
| | Mesh size of $F_A$ ($F_B$) | | | | |
| | 65 mm | 60 mm | 55 mm | 50 mm | 45 mm |
| 0.1 | 2.72 | 2.76 | 2.78 | 2.69 | 2.68 |
| 0.2 | 4.16 | 4.1 | 4.13 | 4.04 | 4.04 |
| 0.3 | 5.88 | 5.58 | 5.69 | 5.64 | 5.56 |
| 0.4 | 7.93 | 7.65 | 7.81 | 7.58 | 7.61 |
| 0.5 | 10.34 | 9.94 | 10.10 | 9.89 | 9.99 |
| 0.65 | 13.44 | 13.11 | 13.27 | 12.88 | 13.14 |
| | Maximum error = (5.88 - 5.58)/5.88*100% =5.10% | | | | |

## Comparison of Simulation Results and Test Results

Figure 6 shows the FEA predicting method for stress-strain of $F_{AB}F$. The compression stress-strain curves of the foam foundation in Fig. 7 can be predicted using fitting parameters of $F_A$, $F_B$, and fabric. The detailed information of stress-strain values between simulation and test results are shown in Table 6.

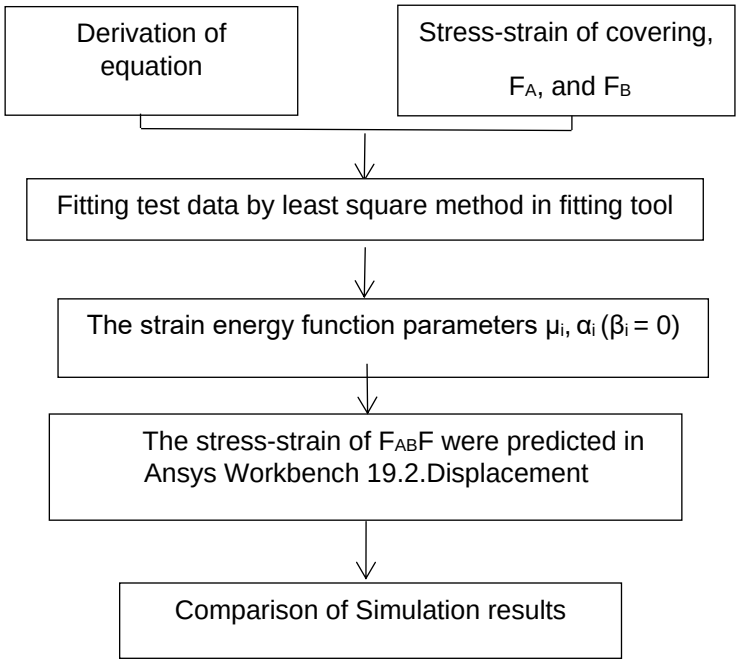


**Fig. 6.** FEA for predicting indentation stress-strain for $F_{AB}F$

**Table 6.** Mean Comparison of FEA Results with Test Results for Stress Values at Each Strain for $F_{AB}F$

| Combination of different elastic material | Test | FEA | % Diff. | Test | FEA | % Diff. | Test | FEA | % Diff. | Test | FEA | % Diff. | Test | FEA | % Diff. | Test | FEA | Percent diff. |
|---|---|---|---|---|---|---|---|---|---|---|---|---|---|---|---|---|---|---|
| | 10% Strain | | | 15% Strain | | | 20% Strain | | | 25% Strain | | | 30% Strain | | | 35% Strain | | |
| $F_{AB}F$ | 1.39 | 2.72 | 95.68 | 3.60 | 3.39 | -5.83 | 5.76 | 4.16 | -27.78 | 6.66 | 5.01 | -24.77 | 7.60 | 5.88 | -22.63 | 8.61 | 6.90 | -19.86 |

| Combination of different elastic material | Test | FEA | % Diff. | Test | FEA | % Diff. | Test | FEA | % Diff. | Test | FEA | % Diff. | Test | FEA | % Diff. | Test | FEA | Percent diff. |
|---|---|---|---|---|---|---|---|---|---|---|---|---|---|---|---|---|---|---|
| | 40% Strain | | | 45% Strain | | | 50% Strain | | | 55% Strain | | | 60% Strain | | | 65% Strain | | |
| $F_{AB}F$ | 9.51 | 7.93 | -16.61 | 10.36 | 9.30 | -10.23 | 11.36 | 10.34 | -8.98 | 12.28 | 11.41 | -7.08 | 13.17 | 12.37 | -6.07 | 14.25 | 13.44 | -5.08 |

The positive and negative signs of individual errors are taken into account when computing the mean Error

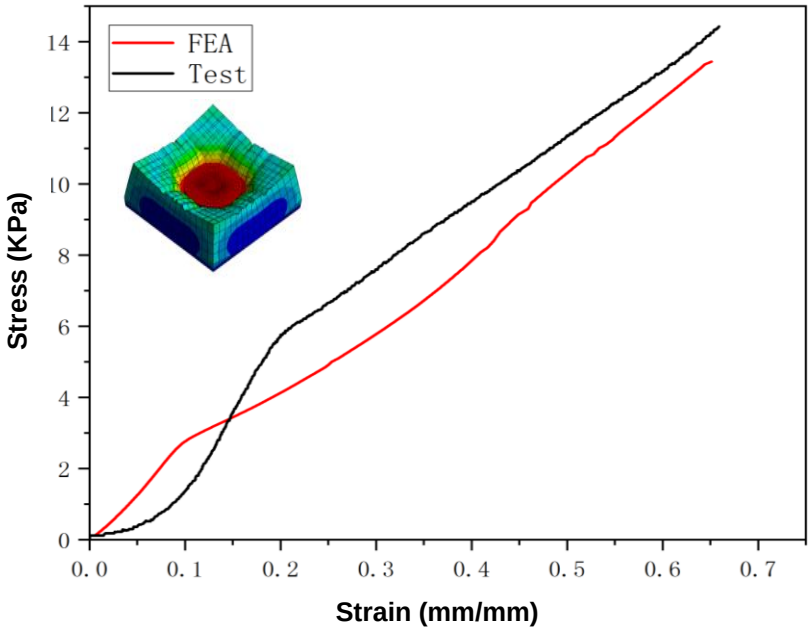


**Fig. 7.** Comparison between FEA results and test results of $F_{AB}F$
(Elements number: 2274; Element quality (average): 0.878; Mesh size of $F_A$ ($F_B$) is 65 mm)

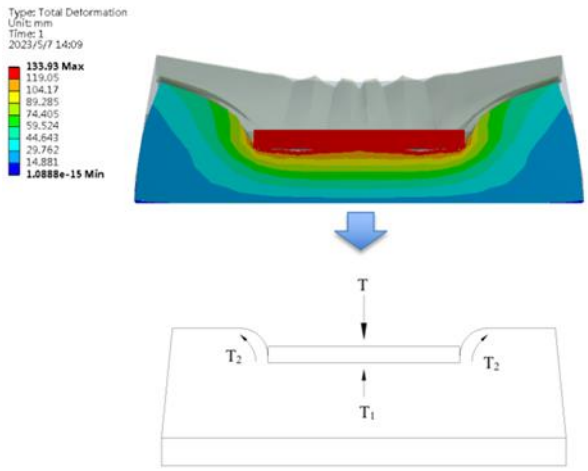


**Fig. 8.** Deformation mechanism of $F_{AB}F$ ($T = T_1 + T_2$)

As shown in Fig. 7, the variation trend of the stress-strain curve in the FEA is consistent with the test results. In addition, Table 6 ($F_{AB}F$) illustrates how the stress inaccuracy decreases from -27.78% to -5.08% when comparing the strain results of 20% to 65%. This might be due to the results of the shear stress (Fig. 8, $T_2$) being disregarded in the simulation during the deformation of polymer foam when the disk is pressed down. When the disk is forced down on a polymer foam, the shear stress (Fig. 8, T2) during the deformation of the polymer foam causes it to deform (Todd *et al*. 1998).

Generally, the stress values typically depend upon the deformation stress of its microunit for elastic materials. Because the $F_A$ or $F_B$ with dimensions of 100 mm × 100 mm × 50 mm (length, breadth, and thickness) were completely covered by the loading head

with a diameter of 200 mm, the experiment data for $F_A$ and $F_B$ through uniaxial compression tests only indicate the foams' axial stress-strain relation ($T_1$), (Fig. 8). However, for the combination of $F_{AB}F$, the dimension is much larger than the compression loading head. In other words, the stress deformation for $F_{AB}F$ occurred at different angles, including $T_1$ and $T_2$ (Fig. 8).

In addition, other original images that caused errors are as follows：

(1) Polymer foams are elastically anisotropic and have complex failure mechanisms.

(2) The FEA material models for polymer foams have the limitations of assuming material isotropy, and the commencement of yielding occurs in a similar manner under a variety of stress states.

(3) The porosity, pore size, and material properties are all crucial in relation to the stress-strain of the polymer foams.

As shown in Table 6 ($F_{AB}F$), the stress error drops from 95.68% to -5.08%, comparing the strain results of 10% to 65%. The maximum error between finite element analysis and experimental testing occurs in the 10% of the strain, and after the first 20% of the strain, the errors gradually stabilized (Fig. 7). This shows how the Ogden model can be used to somewhat predict the elastic behavior of foam seat foundation.

In addition, because the silk wadding was difficult to model and specify in FEA, a layer of low-elasticity foam (50 mm) was used as a substitute at the bottom of the $F_{AB}F$. It has been observed that the FEA results are higher than the test results before 15% strain of the $F_{AB}F$ happened in Fig. 7. This is because the thickness and property of silk wadding of simulation for $F_{AB}F$ is not exactly 50 mm. The stress-strain prediction results of the double-layer polymer foam with covering combination demonstrate the method's logic for the overall trend of curve variation.

## CONCLUSIONS

This study quantified the stress-strain relations of single-layer polymer foams and double-layer polymer foam with covering combination by a uniaxial compression test and FEA.

1. The test data of small polymer foams and covering were fitted by a non-linear least square method based on the Ogden foam and Ogden constitutive equation of Ansys Workbench 19.2, and FEA was used to estimate the stress-strain behavior of foam seat foundation.
2. The stress errors between FEA and test results of foam foundation decreased from 95.68% to -5.08% , when the strain is 10% to 65%.This shows that the variation trend of the stress-strain curve in the FEA is consistent with the test results.

## ACKNOWLEDGMENT

The authors gratefully acknowledge the financial support for the present work from the National Natural Science Foundation of China (Grant No. 52005450).

## REFERENCES CITED

ASTM D3574-B1 (2003). "Standard test methods for flexible cellular materials—Slab, bonded, and molded urethane foams," ASTM International, West Conshohocken, PA, USA.

Briody, C., Duignan, B., and Jerrams, S. (2011). "Testing, modelling, and validation of numerical model capable of predicting stress fields throughout polyurethane foam," in: *7th European Conference on Constitutive models for Rubber (ECCMR)*, Dublin, Ireland.

Briody, C., Duignan, B., and Jerrams, S. (2012). "The implementation of a visco-hyperelastic numerical material model for simulating the behaviour of polymer foam materials," *Computational Materials Science* 64, 47-51. DOI: 10.1016/j.commatsci.2012.04.012

Chen, H., and Cai, L. X. (2018). "An elastoplastic energy model for predicting the deformation behaviors of various structural components," *Applied Mathematical Modelling* 68, 405-421. DOI: 10.1016/j.apm.2018.11.024

Chou, C. C., Zhao, Y., Chai, L., Co, J., Lim, G. G., and Lin, T. L. (1995). "Development of foam models as applications to vehicle interior," *SAE Technical Paper Series* 952733, 335-348. DOI: 10.4271/952733

Chuda-Kowalska, M., Gajewski, T., and Garbowski, T. (2015). "Mechanical characterization of orthotropic elastic parameters of a foam by the mixed experimental-numerical analysis," *Journal of Theoretical & Applied Mechanics* 53(2), 383-394. DOI:10.15632/jtam-pl.53.2.383.

Du, X., Ren, J., Sang, C., and Li, L. (2013). "Simulation of the interaction between driver and seat," *Chinese Journal of Mechanical Engineering* 26(06), 1234-1242. DOI: 10.3901/CJME.2013.06.1234

EN 1957 (2000). "Domestic furniture - Beds and mattresses - Test methods for the determination of functional characteristics," European Committee for Standardization, Brussels, Belgium.

Fernández, J. R., López-Campos, J. A., Segade, A., and Vilan, J. A. (2018). "A genetic algorithm for the characterization of hyperelastic materials," *Applied Mathematics and Computation* 329, 239-250. DOI: 10.1016/j.amc.2018.02.008

Gao, Z., Li, M., Gao, F., Mei, X., Yang, F., and Zhang, H. (2019). "Analysis on effect of foaming density of automotive seats on sitting comfort," *Journal of Hunan University* (Natural Science Edition) 46(10), 19-25. DOI: 10.16339/j.cnki.hdxbzkb.2019.10.003

GB/T 3923.1 (2013). "Textiles—Tensile properties of fabrics—Part 1: Determination of maximum force and elongation at maximum force using the strip method," Standardization Administration of China, Beijing, China.

Heczko, J., and Kottner, R. (2018). "Modeling of material damage using finite elements and time homogenization in case of finite strain," *Applied Mathematics and Computation* 319, 264-273. DOI: 10.1016/j.amc.2017.03.014

Hu, L., Tackett, B., Tor, O., and Zhang, J. (2015). "Analysis of sitting forces on stationary chairs for daily activities," *Ergonomics* 59(4), 1-38. DOI: 10.1080/00140139.2015.1080311

Hu, L., Tor, O., Li, M., Zhang, J., Franklin, Q., and Yu, X. (2020). "Cushioning capability analysis of seat foundations considering the sitter's anthropometric dimensions," *BioResources* 15(4), 7992-8007. DOI: 10.15376/BIORES.15.4.7992-8007

Hu, L., Tor, O., Shen, L., Zhang, J., and Quin, F. (2020). "Cushioning capability analysis of seat foundations considering the sitter's anthropometric dimensions," *BioResources* 15(4), 7992-8007. DOI: 10.15376/biores.15.4.7992-8007

Kumar, V., Mishra, R. K., and Krishnapillai, S. (2019). "Study of pilot's comfortness in the cockpit seat of a flight simulator," *International Journal of Industrial Ergonomics* 71. DOI: 10.1016/j.ergon.2019.02.004

Li, H. (2018). *Study on the Indentation Force Deflection and Support Performance of Elastic Materials of Sofa Cushion*, Dissertation, Zhejiang A&F University, China.

Liu, Q., and Subhash, G. (2004). "A phenomenological constitutive model for foams under large deformations," *Polymer Engineering & Science* 44(3), 463-473. DOI: 10.1002/pen.20041

Liu, Q., Subhash, G., and Gao, X. L. (2005). "A parametric study on crushability of open-cell structural polymeric foams," *Journal of Porous Materials* 12(3), 233-248. DOI: 10.1007/s10934-005-1652-1

Maiti, A., Small, W., Lewicki, J. P., Chinn, S. C., and Wilson, T. S. (2019). "Age-aware constitutive materials model for a 3D printed polymeric foam," *Scientific Reports* 9(1), article 15923. DOI: 10.1038/s41598-019-52298-z

Masrar, Y., and Ettaouil, M. (2021). "A nonlinear plane strain finite element analysis for multilayer elastomeric bearings," *Applied Mathematics and Computation* 404, article ID 126218. DOI: 10.1016/j.amc.2021.126218

Mills, N. J., and Gilchrist, A. (2000). "Modelling the indentation of low density polymer foams," *Cellular Polymers: An International Journal* 19(6), 389-412.

Mohanty, P. P., and Mahapatra, S. S. (2014). "A finite element approach for analyzing the effect of cushion type and thickness on pressure ulcer," *International Journal of Industrial Ergonomics* 44(4), 499-509. DOI: 10.1016/j.ergon.2014.03.003

Ogden, R. W. (1972). "Large deformation isotropic elasticity: On the correlation of theory and experiment for compressible rubberlike solids," *Proceedings of the Royal Society of London. Series A, Mathematical and Physical Sciences* 328(1575), 567-583. DOI: 10.1098/rspa.1972.0096

Ogden, R. W. (1984). "Non-linear elastic deformations," *Engineering Analysis* 1(2), 119. DOI: 10.1016/0264-682X(84)90061-3

Ozturk, U. E., and Anlas, G. (2007). "Multiple compressive loading and unloading behavior of polymeric foams," *Journal of Polymer Engineering* 27(8), 607-619. DOI: 10.1515/POLYENG.2007.27.8.607

Ozturk, U. E., and Anlas, G. (2010). "Finite element analysis of expanded polystyrene foam under multiple compressive loading and unloading," *Materials & Design* 32(2), 773-780. DOI: 10.1016/j.matdes.2010.07.025

Schrodt, M., Benderoth, G., Kühhorn, A., and Silber, G. (2005). "Hyperelastic description of polymer soft foams at finite deformations," *Technische Mechanik* 25(3), 162-173.

Todd, B. A., Smith, S. L., and Vongpaseuth, T. (1998). "Polyurethane foams: Effects of specimen size when determining cushioning stiffness," *Journal of Rehabilitation Research and Development* 35(2), 219-224.

Zeng, W., Yan, J., Hong, Y., and Cheng, S. S. (2021). "Numerical analysis of large deflection of the cantilever beam subjected to a force pointing at a fixed point," *Applied Mathematical Modelling* 92, 719-730. DOI: 10.1016/j.apm.2020.11.023

Zhang, Z., Li, C., Liang, L., Xu, Z., and He, Y. (2019). "Design method of customized cushion contact surface based on body pressure data mapping," *Journal of Mechanical Engineering* 55(17), 162-171.

Zhang, Z., Nie, J., Shen, M., and Xin, Z. (2005). "Hyperelastic model in ANSYS and its application in rubber engineering," *Rubber and Plastic Technology and Equipment* 2005(09), 1-5.

Article submitted: June 29, 2023; Peer review completed: August 5, 2023; Revised version received and accepted: September 4, 2023; Published: September 29, 2023.
DOI: 10.15376/biores.18.4.7731-7744